Macromolecules

Article

pubs.acs.org/Macromolecules

# Thermo-Induced Aggregation and Crystallization of Block Copolypeptoids in Water

Christian Secker,[†] Antje Völkel,[†] Brigitte Tiersch,[‡] Joachim Koetz,[‡] and Helmut Schlaad*[,‡]

[†]Department of Colloid Chemistry, Max Planck Institute of Colloids and Interfaces, Research Campus Golm, 14424 Potsdam, Germany

[‡]Institute of Chemistry, University of Potsdam, Karl-Liebknecht-Straße 24-25, 14476 Potsdam, Germany

Supporting Information

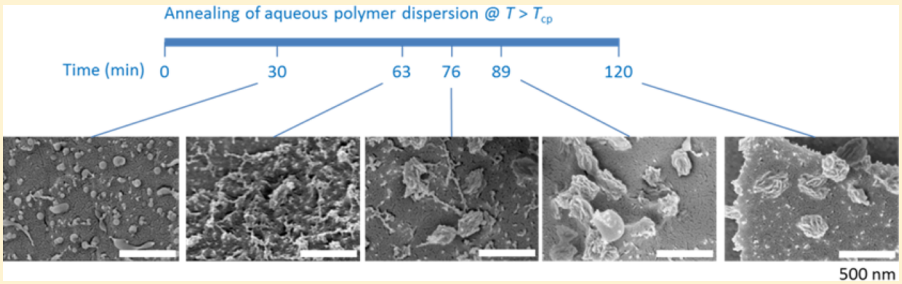


**ABSTRACT:** Block copolypeptoids comprising a thermosensitive, crystallizable poly(*N*-(*n*-propyl)glycine) block and a water-soluble poly(*N*-methylglycine) block, $P_{70}M_y$ ($y$ = 23, 42, 76, 153, and 290), were synthesized by ring-opening polymerization of the corresponding *N*-alkylglycine *N*-carboxyanhydrides (NCAs) and examined according to their thermo-induced aggregation and crystallization in water by turbidimetry, micro-differential scanning calorimetry (micro-DSC), cryogenic scanning electron microscopy (cryo-SEM), analytical ultracentrifugation (AUC), and static light scattering (SLS). At a temperature above the cloud point temperature, the initially formed micellar aggregates started to crystallize and grow into larger complex assemblies of about 100−500 nm, exhibiting flower-like ($P_{70}M_{23}$), ellipsoidal ($P_{70}M_{42}$ and $P_{70}M_{72}$), or irregular shapes ($P_{70}M_{153}$ and $P_{70}M_{290}$).

## INTRODUCTION

Synthetic poly(*N*-alkylglycine)s, also referred to as poly(α-peptoid)s, represent an interesting and versatile class of bio(inspired) materials mimicking polypeptides. The physicochemical properties of polypeptoids, i.e., thermal properties, crystallinity, solubility, etc., and aggregation/self-assembly behavior can be designed by simple variation of the side chains.[1−4] Advanced synthetic procedures[5−9] toward well-defined linear and cyclic polypeptoids have been described as well as detailed studies on solubility properties,[6,10−12] thermoresponsive behavior,[10,13−15] aggregation,[16] and crystallization in aqueous solution[10] and in bulk.[11,17,18] Polypeptoids are considered as biocompatible,[16,19,20] and poly(*N*-methylglycine) (polysarcosine) shows nonfouling properties.[21] Degradation of polypeptoids follows nonenzymatic pathways, for instance by oxidative decomposition under physiological conditions.[22]

These properties make polypeptoid brush polymers or aggregates, micelles or vesicles, prone for biomedical applications such as drug or gene delivery.[23] For this, however, cargo-loaded aggregates need to be stable in a physiological environment, for instance in blood serum, and also stable against dilution. In order to avoid disassembly, the carriers are cross-linked in the core or corona by chemical cross-linking, for instance applying click chemistry[24] or by physical cross-linking through multivalent ions,[25] polyion complexation,[26] or crystallization.[27] Also, frozen micelles, having a glassy core made of a polymer with high glass transition temperature, are potentially suitable carrier systems.

Here, we examine the use of partial crystallization of block copolypeptoid aggregates for the fabrication of stable, physically cross-linked, and hopefully useful carrier systems. Especially crucial (regarding application) but interesting (scientifically) was the question if the crystallization process would preserve the initial aggregate morphology, as has for instance been observed for the stepwise "micellization−crystallization" of polyethylene-*block*-poly(*N*,*N*-dimethylacrylamide),[28] or produce crystalline-core cylindrical micelles and even more complex hierarchical structures through "crystallization-driven self-assembly" (CDSA) or "directional crystallization".[29−35] A series of copolymers consisting of a thermosensitive/crystallizable poly(*N*-(*n*-propyl)glycine)[10] block and a hydrophilic poly(*N*-methylglycine) block varying in composition were synthesized and studied according to their aqueous solution behavior. The thermo-induced formation and crystallization of aggregates were followed by phototurbimetry, micro-differential scanning calorimetry (micro-DSC), and cryogenic scanning electron microscopy (cryo-SEM) as well as by differential

**Received:** November 16, 2015
**Revised:** December 22, 2015





DOI: 10.1021/acs.macromol.5b02481
*Macromolecules* XXXX, XXX, XXX−XXX

scanning calorimetry (DSC), analytical ultracentrifugation (AUC), and static light scattering (SLS).

## EXPERIMENTAL SECTION

**Materials.** *N-tert*-Butyloxycarbonyl(Boc)-*N*-methylglycine (Boc-Sar-OH, ≥99%, Sigma-Aldrich), phosphorous trichloride ($PCl_3$, 99%), glyoxylic acid monohydrate (98%), *n*-propylamine (≥99%), and *n*-heptanes (≥99%) were purchased from Sigma-Aldrich and used as received. Ethyl acetate (EtOAc, 99.5%, Th. Geyer) and methanol (MeOH, LiChrosolv, VWR) were used as received. Anhydrous *N*-methyl-2-pyrrolidone (NMP, 99.5%) and benzonitrile (PhCN, 99%) were purchased from Sigma-Aldrich in septum-sealed bottles over molecular sieves. Benzylamine ($BnNH_2$, 99.5%), acetic anhydride ($Ac_2O$, 99%), dichloromethane (DCM, ≥99.9%), and cyclohexane (cHex, ≥99%), all from Sigma-Aldrich, were distilled from calcium hydride and stored over activated molecular sieves (3 Å; 3−5 mm beads) under argon (flowed through a $CaCl_2$ drying tube). All laboratory equipment was cleaned and flash dried prior to use with a heat gun at reduced pressure (~0.01 mbar).

**Monomer Synthesis.** The *N*-methylglycine (sarcosine) *N*-carboxyanhydride (MeGlyNCA) was obtained in a one-step synthesis from *N*-Boc-*N*-methylglycine (dried under reduced pressure overnight, 10.6 g, 0.056 mol) in anhydrous DCM (350 mL) with $PCl_3$ (added via dropping funnel, 5.86 mL, 0.067 mol) at 0 °C for 6 h. Volatiles were removed by rotoevaporation, and final purification was obtained by sublimation (65 °C, 0.012 mbar, 12 h), yielding a white crystalline material (80−90%); mp 103.2 °C. $^1$H NMR (DMSO-$d_6$, 400 MHz) $\delta$ 4.22 (s, 2H), 2.86 (s, 3H) ppm. GC-MS (MSD) $R_t$ 10.8 min; (EI) $m/z$ 115.0 ($M^+$, $[C_3H_5NO]^+$ = 71.0). The *N*-(*n*-propyl)glycine *N*-carboxyanhydride (PrGlyNCA) was synthesized in three steps, starting from glyoxylic acid and *n*-propylamine, as described elsewhere.[10] The crude product was purified by distillation followed by filtering through silica and washing with EtOAc. After rotoevaporation, the product was redissolved in EtOAc, filtered, and concentrated afterward. cHex was added to the oily product, stirred vigorously, and decanted, and the procedure was repeated (3×) before final drying under reduced pressure (0.012 mbar), yielding a beige, waxy solid (67%); mp <20 °C. $^1$H NMR ($CDCl_3$, 400 MHz): $\delta$ 4.10 (s, 2H), 3.38 (t, 2H), 1.65 (m, 2H), 0.97 (t, 3H) ppm. GC-MS (MSD) $R_t$ 13.7 min; (EI) $m/z$ 143.1 ($M^+$, $[C_5H_9NO]^+$ = 100.1, $[C_2H_2NO]^+$ = 57.1).

**Block Copolypeptoid Synthesis.** A series of five poly(*N*-(*n*-propyl)glycine)$_x$-*block*-poly(*N*-methylglycine)$_y$ ($P_xM_y$) (subscripts denote the average number of repeat units, by $^1$H NMR) were synthesized by sequential nucleophilic ring-opening polymerization of the corresponding NCAs. A batch of poly(*N*-(*n*-propyl)glycine)$_{70}$ (in the following referred to as $P_{70}$) macroinitiator was prepared by adding a 1 M $BnNH_2$/NMP stock solution to a solution of PrGlyNCA (3.79 g) in PhCN (38 mL) ($[NCA]_0/[BnNH_2]_0$ = 60); the mixture was stirred at room temperature under an argon atmosphere and frequently degassed over time. The conversion was monitored by GC-MS and $^1$H NMR, and once all monomer was consumed (after ~48 h) the reaction volume was split into six portions: five for further reactions and one for analysis (→ $P_{70}$ homopolymer, terminated with $Ac_2O$). Volatiles were evaporated, and the crude product was redissolved in MeOH, precipitated in *n*-heptanes, and dialyzed against MeOH (MWCO 3500 Da, regenerated cellulose). After drying, $P_{70}$ was obtained as a white powder; gravimetric yield: 416 mg (95%). $^1$H NMR (DMSO-$d_6$, 600 MHz): $\delta$ 7.36−7.18 (m, 5H), 4.47−3.80 (m, ~139H), 3.40−3.00 (m, ~169H), 1.65−1.25 (d, br, ~144H), 0.95−0.68 (d, br, ~216H) ppm. $^{13}$C NMR (DMSO-$d_6$, 100 MHz): $\delta$ 169.2, 168.3, 128.2, 49.0, 48.0, 21.0, 20.2, 11.1 ppm. SEC (NMP, PMMA calibration): $\bar{M}_n^{app}$ 7.0 kg mol$^{-1}$, $\bar{M}_w^{app}$ 7.4 kg mol$^{-1}$, $(\bar{M}_w/\bar{M}_n)^{app}$ 1.06.

The $P_{70}$ macroinitiator (0.062 mmol) in PhCN (6.4 mL) was added to solutions of MeGlyNCA (1.23−17.3 mmol) in PhCN to obtain ~2.2−10 wt % monomer solutions. The mixtures were stirred for 48 h at room temperature under an argon atmosphere and then quenched with $Ac_2O$ (3 mL). Polymers were purified and isolated (89−94% yield) as described above and analyzed by $^1$H NMR (→ composition, $y$) and SEC (→ apparent molar mass averages and dispersity). $P_{70}M_{23}$: $^1$H NMR (DMSO-$d_6$, 600 MHz): $\delta$ 7.36−7.18 (m, ~5H), 4.47−3.80 (m, ~182H), 3.40−3.00 (m, ~177H), 3.00−2.65 (m, ~70H), 1.65−1.25 (d, br, ~144H), 0.95−0.68 (d, br, ~216H) ppm. $^{13}$C NMR (DMSO-$d_6$, 100 MHz): $\delta$ 169.2, 169.0, 48.9, 48.0, 20.3, 20.1, 11.1 ppm. SEC (NMP, PMMA calibration): $\bar{M}_n^{app}$ 7.7 kg mol$^{-1}$, $\bar{M}_w^{app}$ 8.7 kg mol$^{-1}$, $(\bar{M}_w/\bar{M}_n)^{app}$ 1.13. $P_{70}M_{42}$: $^1$H NMR (DMSO-$d_6$, 600 MHz): $\delta$ 7.36−7.18 (m, ~5H), 4.47−3.80 (m, ~221H), 3.40−3.00 (m, ~170H), 3.00−2.65 (m, ~127H), 1.65−1.25 (d, br, ~143H), 0.95−0.68 (d, br, ~216H) ppm. SEC (NMP, PMMA calibration): $\bar{M}_n^{app}$ 8.7 kg mol$^{-1}$, $\bar{M}_w^{app}$ 10.0 kg mol$^{-1}$, $(\bar{M}_w/\bar{M}_n)^{app}$ 1.15. $P_{70}M_{76}$. $^1$H NMR (DMSO-$d_6$, 600 MHz): $\delta$ 7.36−7.18 (m, ~4H), 4.47−3.80 (m, ~287H), 3.40−3.00 (m, ~173H), 3.00−2.65 (m, ~230H), 1.65−1.25 (d, br, ~144H), 0.95−0.68 (d, br, ~216H) ppm. SEC (NMP, PMMA calibration): $\bar{M}_n^{app}$ 10.0 kg mol$^{-1}$, $\bar{M}_w^{app}$ 11.7 kg mol$^{-1}$, $(\bar{M}_w/\bar{M}_n)^{app}$ 1.17. $P_{70}M_{153}$. $^1$H NMR (DMSO-$d_6$, 600 MHz): $\delta$ 7.36−7.18 (m, ~4H), 4.47−3.80 (m, ~444H), 3.40−3.00 (m, ~257H), 3.00−2.65 (m, ~459H), 1.65−1.25 (d, br, ~145H), 0.95−0.68 (d, br, ~216H) ppm. SEC (NMP, PMMA calibration): $\bar{M}_n^{app}$ 12.7 kg mol$^{-1}$, $\bar{M}_w^{app}$ 14.6 kg mol$^{-1}$, $(\bar{M}_w/\bar{M}_n)^{app}$ 1.15. $P_{70}M_{290}$. $^1$H NMR (DMSO-$d_6$, 600 MHz): $\delta$ 7.36−7.18 (m, ~9H), 4.47−3.80 (m, ~741H), 3.40−3.00 (m, ~347H), 3.00−2.65 (m, ~871H), 1.65−1.25 (d, br, ~148H), 0.95−0.68 (d, br, ~216H) ppm. SEC (NMP, PMMA calibration): $\bar{M}_n^{app}$ 14.3 kg mol$^{-1}$, $\bar{M}_w^{app}$ 16.9 kg mol$^{-1}$, $(\bar{M}_w/\bar{M}_n)^{app}$ 1.18.

**Analytical Instrumentation and Methods.** Melting points were determined with a MEL-TEMP II apparatus (Laboratory Devices Inc. (USA)) in open glass capillaries. Purity of low molecular weight compounds and monomer conversion was examined with gas chromatography−mass spectrometry (GC-MS) using an Agilent Technologies GC 6890N MS 5975. Aliquots of the polymerization solution were diluted with $CHCl_3$ at concentrations of 1−10 mg mL$^{-1}$ and prepared in 2 mL septum-sealed vials. The Enhanced ChemStation software was used to set following measurement parameters: A sample volume of 1 $\mu$L was injected into the preheated chamber (250 °C), split (10:1), and flowed (He; 0.76 bar) through the heated (30−300 °C; 2 min hold, then 30 K min$^{-1}$) column. Data were acquired after 3 min of solvent delay (duration of 11.33 min), and subsequently the aforementioned software was used to analyze the chromatogram. Nuclear magnetic resonance (NMR) spectroscopy was conducted with a Bruker DPX-400 or Varian 600 MHz device at room temperature. Samples of ~5−25 mg mL$^{-1}$ concentrations were prepared in $CDCl_3$ or DMSO-$d_6$ (Aldrich). Signals were referenced to signals of residual protonated solvent: $CDCl_3$: $\delta$ $^1$H 7.26 ppm, $^{13}$C 77.0 ppm; DMSO-$d_6$: $\delta$ $^1$H 2.50 ppm, $^{13}$C 39.5 ppm. Size exclusion chromatography (SEC) was performed in NMP (+ 0.5 wt % LiBr) as eluent at +70 °C, flow rate: 0.8 mL min$^{-1}$, utilizing simultaneous UV ($\lambda$ = 270 nm) and RI detection. The stationary phase consisted of two 300 × 8 mm$^2$ PSS-GRAM columns (7 $\mu$m spherical polyester particles) columns with porosities of $10^2$ and $10^3$ Å. Solutions containing ~0.15 wt % polymer were filtered through 0.45 $\mu$m filters (GF/F Whatman); the injected volume was 100 $\mu$L. Calibration curve was recorded with poly(methyl methacrylate) (PMMA) standards. Data analysis was done with the PSS WinGPC software (Polymer Standards Service (PSS) GmbH, Mainz, Germany). Analytical ultracentrifugation (AUC) measurements were conducted using an Optima XL-I analytical ultracentrifuge (Beckman Coulter, Palo Alto, CA) equipped with a Rayleigh interference optics. A four-hole titanium rotor was operated at 25 °C and 1500/5000/20 000 and 60 000 rpm. The samples (0.15 wt % aqueous solutions) were filled in 12 mm double sector center pieces made from titanium (Nanolytics, Potsdam, Germany). Sedimentation coefficient distributions were evaluated by the least-squares $g^*(s)$ (ls $g^*(s)$) evaluation using the SEDFIT software package.[36] Turbidimetric measurements were conducted with a turbidimetric photometer TP1 (Tepper Analytik, Wiesbaden, Germany) operating at $\lambda$ = 670 nm. Stirred samples were and analyzed between 5 and 95 °C at a heating rate of 0.1 K min$^{-1}$. The sample chamber was purged with nitrogen to prevent condensation onto the quartz cuvettes below room temperature. Micro-differential scanning calorimetry (micro-DSC) was performed using a MicroCal VP-DSC MicroCalorimeter (−10 to +130 °C, short-term noise 0.5 $\mu$cal K$^{-1}$; MicroCal, GE Healthcare and Life Science,


DOI: 10.1021/acs.macromol.5b02481
Macromolecules XXXX, XXX, XXX−XXX

Scheme 1. Synthesis of the Block Copolypeptoid Samples Used in This Work (Bn = Benzyl, Ac = Acetyl)

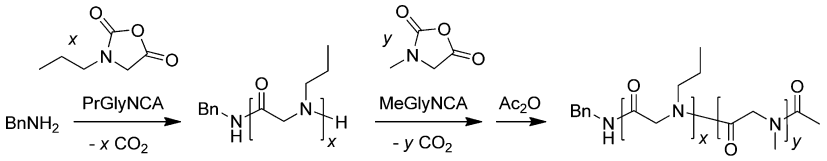


Table 1. Molecular Characteristics of Poly(*N*-(*n*-propyl)glycine)$_{70}$−Poly(*N*-methylglycine)$_y$ ($P_{70}M_y$) Block Copolypeptoids Used in This Work

| sample | $w_M$ [a,h] | $x$ [b,h] | $y$ [c,h] | $y^{cal}$ [d] | $M_n$ (kg mol$^{-1}$) [e,h] | $M_n^{app}$ (kg mol$^{-1}$) [f,i] | $(M_w/M_n)^{app}$ [g,i] |
|---|---|---|---|---|---|---|---|
| $P_{70}$ | | 70 | | | 7.1 | 7.0 | 1.05 |
| $P_{70}M_{23}$ | 0.19 | 70 | 23 | 20 | 8.7 | 7.7 | 1.12 |
| $P_{70}M_{42}$ | 0.30 | 70 | 42 | 37 | 10.1 | 8.7 | 1.14 |
| $P_{70}M_{76}$ | 0.43 | 70 | 76 | 70 | 12.5 | 10.0 | 1.17 |
| $P_{70}M_{153}$ | 0.60 | 70 | 153 | 140 | 18.0 | 12.7 | 1.15 |
| $P_{70}M_{290}$ | 0.74 | 70 | 290 | 280 | 27.7 | 14.2 | 1.18 |

[a]Hydrophilic weight fraction of *N*-methylglycine, $w_M = 71 \cdot y/M_n$ (/g mol$^{-1}$). [b]Average number of *N*-(*n*-propyl)glycine units determined by $^1$H NMR end-group analysis, $x$ = (integral(−C(O)C$\underline{H}_2$N-)/2)/(integral(−$C_6\underline{H}_5$)/5). [c]Average-number of *N*-methylglycine units. [d]Calculated number of *N*-methylglycine units from monomer-to-initiator ratio, $y^{cal} = [NCA]_0/[P_{70}]_0$. [e]Number-average molar mass. [f]Apparent number-average molar mass. [g]Apparent dispersity index. [h]Determined by $^1$H NMR. [i]Determined by SEC with PMMA calibration.

UK). Samples were degassed and measured in comparison to a reference cell filled with Millipore water at a heating/cooling rate of 0.1 K min$^{-1}$ (8−85 °C). High-resolution cryogenic scanning electron microscopy (cryo-SEM) was performed with a Cryo-SEM-4800 (Hitachi, Tokyo, Japan), equipped with a GATAN Alto 2500 cryo-transfer system. A 10 μL aliquot of 1 wt % aqueous solutions were placed in between sandwich sample holders and shock frozen in liquid propane and subsequently transferred into the preparation chamber. The samples were freeze fractured, etched for 45 s at −98 °C, sputtered with platinum, and analyzed with 2 kV acceleration voltages. Static light scattering (SLS) was performed at 25 °C using an ALV-7004 multiple-tau digital correlator in combination with a CGS-3 compact goniometer and a He−Ne laser (Polytec, 34 mW, $\lambda$ = 633 nm). Solutions at 0.01−0.1 wt % were filtered through 0.7 μm syringe filters (GF/F Whatman) and measured at scattering angles from 30° to 150° in 10° steps. Refractive index increments (d$n$/d$c$) measurements were measured with PSS DnDc2010 device operating at $\lambda$ = 620 nm. Differential scanning calorimetry (DSC) was done with Mettler Toledo DSC1/TC100 at heating/cooling rates of 1 K min$^{-1}$ under a nitrogen atmosphere.

**Sample Preparation.** Amorphous polymer samples were obtained by drying a methanolic polymer solution in vacuum (0.012 mbar); complete removal of MeOH was confirmed by $^1$H NMR. Samples for the characterization of thermally annealed, crystalline aggregates in aqueous solution were prepared as follows: amorphous polymer samples were dissolved in chilled (2−5 °C) Millipore water at concentration of 1 wt %. Solutions were filtered through 0.7 μm syringe filters and were kept in septum-sealed, dust-free, light scattering cuvettes at 80 °C for 66 h. Diluted samples were obtained from these stock solutions and Millipore water filtered through 0.7 μm filters.

## RESULTS AND DISCUSSION

**Block Copolypeptoid Synthesis.** A series of five poly(*N*-(*n*-propyl)glycine)$_{70}$-*block*-poly(*N*-methylglycine)$_y$ ($P_{70}M_y$, $y$ = 23, 42, 76, 153, and 290; $M_w/M_n$ < 1.2) were synthesized by sequential nucleophilic ring-opening polymerization of PrGlyNCA and MeGlyNCA (Scheme 1); the molecular characteristics of the samples are listed in Table 1. Characterization by $^1$H NMR (see exemplary spectrum in Figure S1, Supporting Information) supported the chemical structure, high purity, and good agreement between calculated and experimental molar mass ($M_n$). SEC analysis confirmed the absence of homopolymer impurity ($P_{70}$ macroinitiator) in the copolymer samples and narrow molar mass distributions (see see Figure S1).

**Solubility and Thermal Properties.** Poly(*N*-methylglycine) (polysarcosine)[37] is highly soluble in water at room temperature (reported to be miscible with water at all ratios),[6] and poly(*N*-(*n*-propyl)glycine) is soluble at ∼2 wt % (i.e., 20 g L$^{-1}$).[10] Other than poly(*N*-methylglycine), the poly(*N*-(*n*-propyl)glycine) shows thermoresponsive LCST (= lower critical solution temperature) behavior at ambient pressure and crystallization in hot water.[10] The block copolypeptoids of the series $P_{70}M_y$ ($y$ = 23, 42, 76, 153, and 290) are therefore expected to dissolve on a molecular level at room temperature and assemble into core−shell aggregates upon heating to above the cloud point temperature ($T_{cp}$) of the P block (→ aggregates with hydrophobic, dehydrated P core, and hydrophilic M shell). Further annealing of the aggregates would then initiate the crystallization process within the hydrophobic P core.

Aqueous solutions of $P_{70}$ and $P_{70}M_y$ at 1 wt % were analyzed by turbidimetric and micro-DSC measurements (heating rate: 0.1 K min$^{-1}$); results are summarized in Figure 1. The cloud point temperature ($T_{cp}$, referred to the temperature at 80% transmittance) of the $P_{70}$ solution was found to be ∼27 °C, which coincides with an endothermic peak at ∼31 °C (onset at ∼27 °C) in micro-DSC. It has been shown for other LCST-type thermoresponsive systems like poly(*N*-isopropylacrylamide)s[38−40] and poly(2-isopropyl-2-oxazoline)s[41] that the onset of the endothermic transition observed by micro-DSC matches with the cloud point temperature determined by turbidimetry. The micro-DSC results reveal another, exothermic transition at ∼48 °C, which can be attributed to crystallization of the polymer rich phase. This particular sample was freeze-dried and probed by standard DSC, which revealed a glass transition at $T_g$ ∼ 58 °C and a melting transition at $T_m$ ∼ 194 °C (see Figure S2), in accordance with literature values.[10,18]

Turbidimetric and micro-DSC analyses reveal more complex phase behavior for $P_{70}M_y$ block copolypeptoids (see Figure 1). The cloud point transition gets less pronounced the more hydrophilic is the sample; the transmittance drops to 0% at ∼31 °C ($T_{cp}$ ∼ 27 °C) for $P_{70}M_{23}$ and to just 92% at ∼41 °C for


DOI: 10.1021/acs.macromol.5b02481
Macromolecules XXXX, XXX, XXX−XXX

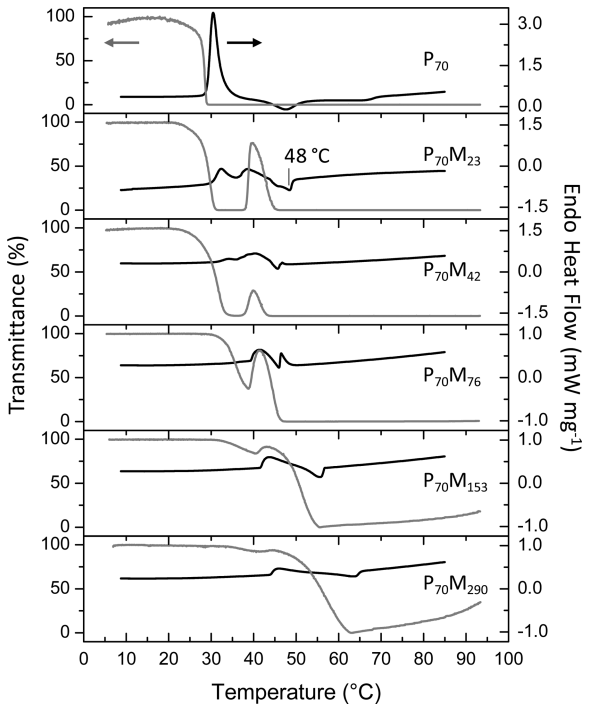


**Figure 1.** Turbimetry (gray lines, left) and micro-DSC first heating curves (black lines, right) of the $P_{70}M_m$ block copolypeptoids at 1 wt % in water (heating rate: 0.1 K $min^{-1}$).

$P_{70}M_{290}$. Afterward the solutions get clearer again, i.e., transmittance increases, at temperatures of 41−45 °C, followed by a second clouding, i.e., transmittance drops to 0%, at 43−63 °C (shifted to higher temperature with increasing length of hydrophilic M block). Exemplary for $P_{70}M_{23}$, the first drop in transmittance at ∼31 °C (turbidimetry) coincides with an endotherm at ∼33 °C (micro-DSC), which is attributed to the dehydration and collapse of the P block. The clearance of the solution at ∼40 °C (turbidimetry) is accompanied by another endothermic signal at ∼39 °C (micro-DSC), indicating the formation of aggregates with supposedly an M shell and a P core.[42,43] After the second clouding (turbidimetry), crystallization of the P core occurs which is an exothermic process (micro-DSC). Subsequent DSC analysis of the freeze-dried specimen showed a melting transition at $T_m$ ∼ 194 °C (Figure S2), verifying the semicrystallinity of the sample (the same was found for all other samples, $T_m$ ∼ 185−195 °C) (Table S1).

The optical appearance of the thermally annealed samples (1 wt % dispersions) ranged from turbid ($P_{70}M_{23}$ and $P_{70}M_{42}$) to opaque ($P_{70}M_{76}$) to opalescent ($P_{70}M_{153}$ and $P_{70}M_{290}$). Coagulation of the $P_{70}M_{23}$ and $P_{70}M_{42}$ dispersions occurred after 1 or 2−3 days, respectively; both samples could be redispersed by shaking and remained stable for the same time span. All other dispersions were colloidally stable for several weeks without noticeable precipitation. The observed behavior of the $P_{70}M_y$ dispersions can be explained by the increasing hydrophilic weight fraction ($w_M$) or length of the poly(*N*-methylglycine) (M) block in the stabilizing shell of the aggregates.

**Characterization of Thermally Annealed Aggregates.** The stable 1 wt % $P_{70}M_y$ dispersions were further analyzed by AUC (diluted to 0.15 wt % with water) and cryo-SEM; results are shown in Figure 2.

According to AUC, the dispersions of $P_{70}M_{23}$, $P_{70}M_{42}$, and $P_{70}M_{76}$ contained only a fast sedimenting species with sedimentation coefficients of $s$ ∼ 5800, 530, and 330 S, respectively; single polymer chains or small aggregates could not be detected (Figure 2A). The large $s$ values indicate that the species exhibit high density (as compared to water) and/or large size. The semicrystalline polypeptoid aggregates can be expected to have a relatively high density (>1.2 g $cm^{-3}$, not confirmed), and their sizes are in the range of ∼400−500 nm ($P_{70}M_{23}$) and 100−200 nm ($P_{70}M_{42}$ and $P_{70}M_{76}$), as evidenced by cryo-SEM (Figure 2B). Hence, the aggregate fraction in AUC seems to correspond to the aggregates seen in cryo-SEM. However, the crystallized aggregates do not exhibit a simple core−shell structure but have a spherical flower-like (rosebud) or ellipsoidal shape (aspect ratio ∼2), similar to the complex structures of crystallized poly(*N*-(*n*-propyl)glycine)[10] and poly(2-alkyl-2-oxazoline)s.[44,45]

AUC analyses of the $P_{70}M_{153}$ and $P_{70}M_{290}$ dispersions, on the other hand, revealed two main fractions: a fast sedimenting fraction ($s$ ∼ 800 S) of large crystallized aggregates (two or more different species) and a very slow sedimenting fraction ($s$ ∼ 0.7 S) of supposedly small aggregates or single polymer chains (amounting to 3.6 and 17.4 wt %, respectively, as estimated from the interference detector fringes) (Figure 2A). The presence of small aggregates/polymer chains in these two dispersions might arise from the increased chain length (or $w_M$) and stabilizing ability of the water-soluble M block. The large aggregates exhibit a roughly ellipsoidal ($P_{70}M_{153}$) or irregular elongated shape ($P_{70}M_{290}$) and are about 200−400 nm in size (cryo-SEM) (Figure 2B).

The thermally annealed $P_{70}M_y$ dispersions (0.01−0.1 wt %; prepared from the same stock solutions as used for AUC and cryo-SEM) were further analyzed by SLS; results are summarized in Table 2 (the corresponding Guinier plots are shown in Figure S3). Here, only the $P_{70}M_{23}$, $P_{70}M_{42}$, and $P_{70}M_{76}$ dispersions, which contained only larger uniform aggregates and no free polymer chains (AUC), were examined.

**Table 2. Static Light Scattering (SLS) Results for Aqueous Dispersions of Thermally Annealed $P_{70}M_{23}$, $P_{70}M_{42}$, and $P_{70}M_{76}$**

| sample | $R_g$ (nm)[a] | $A_2$ (mol $dm^2$ $g^{-2}$)[b] | $M_w^{app}$(kg $mol^{-1}$)[c] | $N_{agg}$[d] |
|---|---|---|---|---|
| $P_{70}M_{23}$ | 217 | $1.18 \times 10^{-8}$ | $1.26 \times 10^5$ | 14610 |
| $P_{70}M_{42}$ | 75 | $5.97 \times 10^{-8}$ | $2.90 \times 10^3$ | 290 |
| $P_{70}M_{76}$ | 80 | $2.59 \times 10^{-8}$ | $5.70 \times 10^3$ | 490 |

[a]Radius of gyration. [b]Second virial coefficient. [c]Apparent weight-average molar mass of aggregates. [d]Aggregation number, $N_{agg} = M_w^{app}/M_w^{polymer} = M_w^{app}/[M_n(M_w/M_n)^{app}]$ (see Table 1).

The radii of gyration ($R_g$) of the aggregates determined by SLS seem to correspond to the aggregate sizes observed in cryo-SEM (Figure 2B). The largest aggregates of $P_{70}M_{23}$ ($R_g$ ∼ 217 nm) comprise ∼14 610 polymer chains ($N_{agg}$), which indicates that the aggregates do not have a compact but an open structure, which is accordance with the large flower-like morphology described above. The aggregates of $P_{70}M_{42}$ and $P_{70}M_{76}$ are much smaller, $R_g$ ∼ 75−80 nm, and are built of about 290−490 chains. Such low aggregation numbers are in accordance with the smaller non-space-filling, ellipsoidal structures seen in cryo-SEM.

It is worth to be mentioned that the values of the second virial coefficient ($A_2$) are close to zero (Table 2), identifying


DOI: 10.1021/acs.macromol.5b02481
Macromolecules XXXX, XXX, XXX−XXX

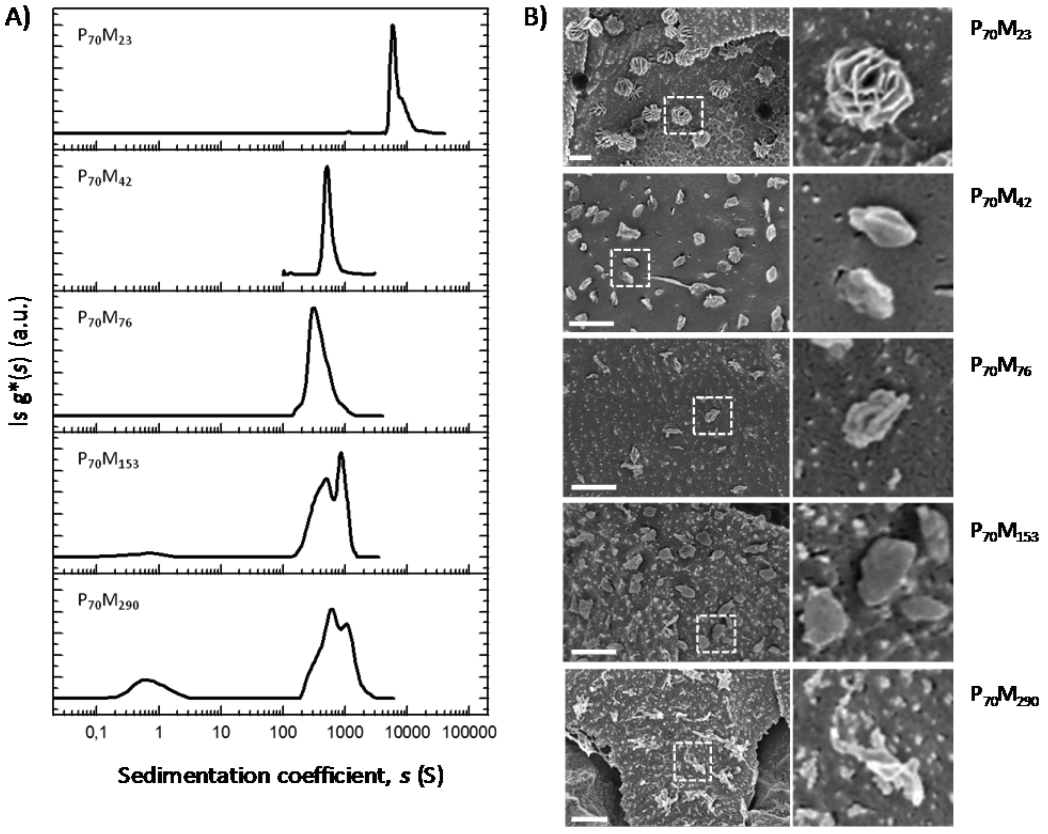


**Figure 2.** Analyses of aqueous dispersions of thermally annealed $P_{70}M_y$ aggregates: (A) AUC sedimentation coefficient distributions (0.15 wt % dispersions). (B) Left: cryo-SEM images (1 wt % dispersions); scale bars = 0.5 $\mu$m. Right: digitally blown-up images of the boxed areas.

water as a theta solvent (note that the outer surface of crystallized aggregates is covered with poly(*N*-methylglycine), as confirmed by $^1$H NMR (data not shown)). Also, the crystallized aggregates were stable against dilution down to 0.01 wt % in water and acidified water but readily dissolved in warm methanol or ethanol.

**Evolution of Crystalline Aggregate Morphology.** Exemplarily, the 1 wt % dispersion of $P_{70}M_{23}$ was subjected to isothermal solvent-mediated crystallization at 48 °C, i.e., the peak temperature of the crystallization process observed in the micro-DSC dynamic scan (see Figure 1), to monitor the evolution of the aggregate morphology after phase separation and during the crystallization process. The isothermal micro-DSC curve and the cryo-SEM images of aliquots taken after distinct annealing times are shown in Figure 3. After 30 min at 48 °C, which is above $T_{cp}$ (= 31 °C, Figure 1), prior to crystallization (micro-DSC, Figure 3A), the P block of $P_{70}M_{23}$ chains should be collapsed and aggregates be formed. Cryo-SEM (Figure 3B) suggests that these aggregates are spherical micelles measuring about 50 nm in diameter. The estimated thickness of the M shell is ~8 nm (assuming fully stretched, all-trans $M_{23}$ segments), and the diameter of the P core is ~34 nm; hence, these micelles should be "crew-cut" micelles.[46] The micelles then start to crystallize to form fibrous intermediates ($t$ = 63 min, first exotherm peak in micro-DSC), which continue to grow in two dimensions to form platelets ($t$ = 76 and 89 min, second exotherm peak in micro-DSC). The platelets fuse together into 3D assemblies of about 250 nm, which mature to give the final spherical flower-like morphology ($t$ = 120 min, cf. Figure 2B). It is interesting to note that very similar crystallized assemblies ($P_{70}M_{23}$; Figures 2A and 3B) were produced from two different processing protocols: (i) heating from 8 to 85 °C at 0.1 K min$^{-1}$ and (ii) constant heating at 48 °C for 120 min.

Although the details of the $P_{70}M_y$ crystallization, which is a nonequilibrium process, are not fully understood yet, there appear to be peculiar differences to the "micellization–crystallization"[28] and the "crystallization-driven self-assembly" processes.[32] That is the initial $P_{70}M_y$ aggregate morphology (spherical micelle) is not preserved but severely altered during the crystallization process, and the crystallized aggregates do not have a simple core–shell structure (like a spherical or cylindrical micelle or vesicle). The stabilizing block appears to have some impact on the final aggregate size and structure (Figure 2B; note that P homopolymer crystals can grow to much larger, micron-sized flower-like particles[10]); however, it can neither avoid the crystallization-driven collapse of the initial aggregate nor prevent crystallization of the P block in 2D (→ platelets) rather than 1D (→ fibers) to 0D (→ spheres). Other control parameters are the annealing time and temperature, temperature profiles, concentration, additives, etc., which need to be further explored (work in progress).

As a matter of fact, the $P_{70}M_y$ block copolypeptoids exhibit an interesting thermo-induced aggregation/crystallization behavior in water, resulting in stable anisotropic aggregates with complex structures; however, these may not be readily used as a drug carrier.

## ■ CONCLUSIONS

Block copolypeptoids comprising a thermosensitive, crystallizable poly(*N*-(*n*-propyl)glycine) block and a water-soluble poly(*N*-methylglycine) block, $P_{70}M_y$ ($y$ = 23–290), were synthesized by ring-opening polymerization of the correspond-


DOI: 10.1021/acs.macromol.5b02481
*Macromolecules* XXXX, XXX, XXX–XXX

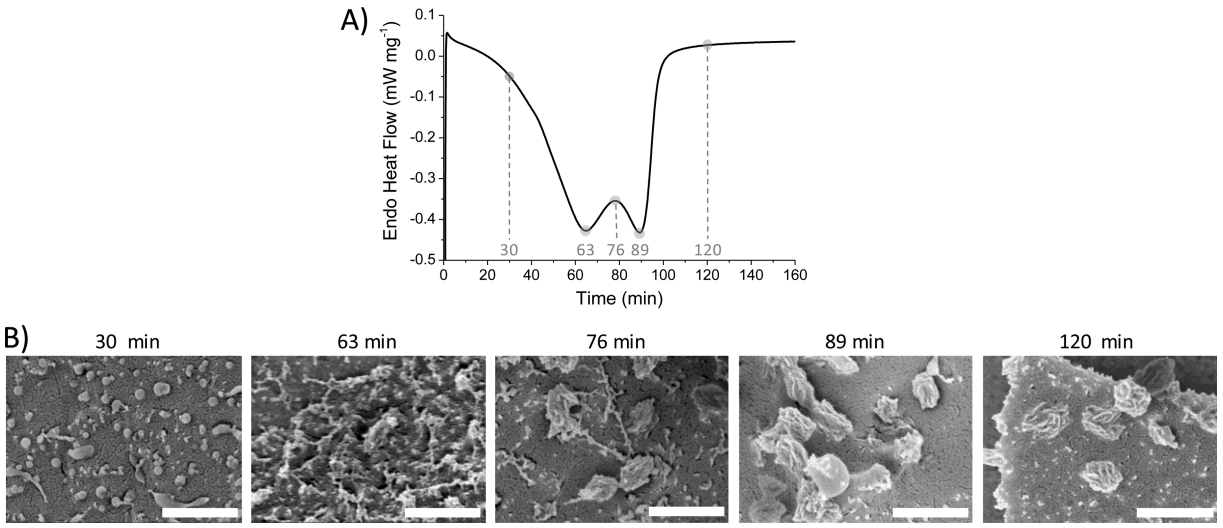


**Figure 3.** (A) Isothermal micro-DSC curve of the 1 wt % aqueous dispersion of $P_{70}M_{23}$ at 48 °C. (B) Cryo-SEM images of the thermally annealed dispersion at $t$ = 30, 63, 76, 89, and 120 min; scale bars = 0.5 $\mu$m.

ing *N*-alkylglycine NCAs and examined according to their thermo-induced aggregation (micellization) and subsequent crystallization in aqueous solution. The aggregation/crystallization processes were studied with turbidimetry and micro-DSC, and the formed aggregate structures were imaged with cryo-SEM. The aqueous dispersions of crystallized aggregates were further characterized by AUC and SLS analyses.

Initially, at a temperature above the cloud point temperature, spherical micelles of 50 nm in diameter were formed (as confirmed for $P_{70}M_{23}$ as the least hydrophilic sample), which upon annealing and crystallization transformed into fibrous intermediates and further grew into platelets. These platelets assembled into larger complex 3D structures, measuring ~100−500 nm (cryo-SEM and SLS), exhibiting flower-like ($P_{70}M_{23}$), ellipsoidal ($P_{70}M_{42}$ and $P_{70}M_{72}$), or irregular shapes ($P_{70}M_{153}$ and $P_{70}M_{290}$). Evidently, the hydrophilic polypeptoid block had impact on the size and shape of the larger aggregates but was not sufficient to confine the crystallization process. Further to be mentioned that the thermally annealed 1 wt % dispersions were usually stable for days or even weeks, and the crystallized aggregates were stable against dissolution but could be dissolved in methanol or ethanol.

Future work is devoted to the deeper understanding of the thermo-induced aggregation and crystallization processes and fine-tuning of the experimental parameters (annealing time and temperature, temperature profiles, concentration, etc.) in order to produce discrete polypeptoid particles with core−shell structure for potential biomedical use (the crystallinity of the hydrophobic core should be reduced as much as needed to achieve a sufficient stabilization of the aggregates while retaining their initial morphology and also to facilitate the loading of the core with hydrophobic cargo molecules) or higher-order hierarchical structures.

## ■ ASSOCIATED CONTENT

### Supporting Information

The Supporting Information is available free of charge on the ACS Publications website at DOI: 10.1021/acs.macromol.5b02481.

Figures S1−S3 and Table S1 (PDF)

## ■ AUTHOR INFORMATION

### Corresponding Author

*E-mail schlaad@uni-potsdam.de (H.S.).

### Notes

The authors declare no competing financial interest.

## ■ ACKNOWLEDGMENTS

Rumina Dimova, Jens Weber, Jessica Brandt, Marlies Gräwert, Olaf Niemeyer, and Carmen Remde (MPI-KG) are thanked for their contributions to this work. Günter Reiter (University of Freiburg, Germany) and A. Levent Demirel (Koç University, Istanbul, Turkey) are gratefully acknowledged for stimulating discussions on polymer crystallization. Financial support was given by the Max Planck Society and the University of Potsdam.

## ■ REFERENCES

(1) Zhang, D.; Lahasky, S. H.; Guo, L.; Lee, C.-U.; Lavan, M. *Macromolecules* **2012**, *45*, 5833.
(2) Luxenhofer, R.; Fetsch, C.; Grossmann, A. *J. Polym. Sci., Part A: Polym. Chem.* **2013**, *51*, 2731.
(3) Sun, J.; Zuckermann, R. N. *ACS Nano* **2013**, *7*, 4715.
(4) Secker, C.; Brosnan, S. M.; Luxenhofer, R.; Schlaad, H. *Macromol. Biosci.* **2015**, *15*, 881.
(5) Lahasky, S. H.; Serem, W. K.; Guo, L.; Garno, J. C.; Zhang, D. *Macromolecules* **2011**, *44*, 9063.
(6) Fetsch, C.; Grossmann, A.; Holz, L.; Nawroth, J. F.; Luxenhofer, R. *Macromolecules* **2011**, *44*, 6746.
(7) Fetsch, C.; Luxenhofer, R. *Macromol. Rapid Commun.* **2012**, *33*, 1708.
(8) Robinson, J. W.; Schlaad, H. *Chem. Commun.* **2012**, *48*, 7835.
(9) Tao, X.; Deng, Y.; Shen, Z.; Ling, J. *Macromolecules* **2014**, *47*, 6173.
(10) Robinson, J. W.; Secker, C.; Weidner, S.; Schlaad, H. *Macromolecules* **2013**, *46*, 580.
(11) Guo, L.; Zhang, D. H. *J. Am. Chem. Soc.* **2009**, *131*, 18072.
(12) Lee, C. U.; Smart, T. P.; Guo, L.; Epps, T. H.; Zhang, D. H. *Macromolecules* **2011**, *44*, 9574.
(13) Lahasky, S. H.; Hu, X.; Zhang, D. *ACS Macro Lett.* **2012**, *1*, 580.
(14) Lee, C.-U.; Lu, L.; Chen, J.; Garno, J. C.; Zhang, D. *ACS Macro Lett.* **2013**, *2*, 436.
(15) Tao, X.; Du, J.; Wang, Y.; Ling, J. *Polym. Chem.* **2015**, *6*, 3164.



DOI: 10.1021/acs.macromol.5b02481
*Macromolecules* XXXX, XXX, XXX−XXX

(16) Fetsch, C.; Flecks, S.; Gieseler, D.; Marschelke, C.; Ulbricht, J.; van Pée, K.-H.; Luxenhofer, R. *Macromol. Chem. Phys.* **2015**, *216*, 547.
(17) Lee, C.-U.; Li, A.; Ghale, K.; Zhang, D. *Macromolecules* **2013**, *46*, 8213.
(18) Fetsch, C.; Luxenhofer, R. *Polymers* **2013**, *5*, 112.
(19) Maurer, P. H.; Subrahmanyam, D.; Katchalski, E.; Blout, E. R. *J. Immunol.* **1959**, *83*, 193.
(20) Tanisaka, H.; Kizaka-Kondoh, S.; Makino, A.; Tanaka, S.; Hiraoka, M.; Kimura, S. *Bioconjugate Chem.* **2008**, *19*, 109.
(21) Lau, K. H. A.; Ren, C.; Sileika, T. S.; Park, S. H.; Szleifer, I.; Messersmith, P. B. *Langmuir* **2012**, *28*, 16099.
(22) Ulbricht, J.; Jordan, R.; Luxenhofer, R. *Biomaterials* **2014**, *35*, 4848.
(23) Hortz, C.; Birke, A.; Kaps, L.; Decker, S.; Wächtersbach, E.; Fischer, K.; Schuppan, D.; Barz, M.; Schmidt, M. *Macromolecules* **2015**, *48*, 2074.
(24) Ten Brummelhuis, N.; Schlaad, H. *Polym. Chem.* **2011**, *2*, 1180.
(25) Kim, J. O.; Kabanov, A. V.; Bronich, T. K. *J. Controlled Release* **2009**, *138*, 197.
(26) Kataoka, K.; Harada, A.; Nagasaki, Y. *Adv. Drug Delivery Rev.* **2001**, *47*, 113.
(27) Glover, A. L.; Nikles, S. M.; Nikles, J. A.; Brazel, C. S.; Nikles, D. E. *Langmuir* **2012**, *28*, 10653.
(28) Yin, L.; Lodge, T. P.; Hillmyer, M. A. *Macromolecules* **2012**, *45*, 9460.
(29) Wang, X.; Guerin, G.; Wang, H.; Wang, Y.; Manners, I.; Winnik, M. A. *Science* **2007**, *317*, 644.
(30) Gädt, T.; Ieong, N. S.; Cambridge, G.; Winnik, M. A.; Manners, I. *Nat. Mater.* **2009**, *8*, 144.
(31) Qiu, H.; Hudson, Z. M.; Winnik, M. A.; Manners, I. *Science* **2015**, *347*, 1329.
(32) Schmelz, J.; Schacher, F. H.; Schmalz, H. *Soft Matter* **2013**, *9*, 2101.
(33) Demirel, A. L.; Meyer, M.; Schlaad, H. *Angew. Chem., Int. Ed.* **2007**, *46*, 8622.
(34) Legros, C.; De Pauw-Gillet, M.-C.; Tam, K. C.; Taton, D.; Lecommandoux, S. *Soft Matter* **2015**, *11*, 3354.
(35) Rudolph, T.; Lühe, M. v. d.; Hartlieb, M.; Norsic, S.; Schubert, U. S.; Boisson, C.; D'Agosto, F.; Schacher, F. H. *ACS Nano* **2015**, *9*, 10085.
(36) Schuck, P. *Biophys. J.* **2000**, *78*, 1606.
(37) Fasman, G. D.; Blout, E. R. *Biopolymers* **1963**, *1*, 99.
(38) Schild, H. G.; Tirrell, D. A. *Langmuir* **1991**, *7*, 665.
(39) Principi, T.; Goh, C. C. E.; Liu, R. C. W.; Winnik, F. M. *Macromolecules* **2000**, *33*, 2958.
(40) Cao, Z. Q.; Liu, W. G.; Gao, P.; Yao, K. D.; Li, H. X.; Wang, G. C. *Polymer* **2005**, *46*, 5268.
(41) Diab, C.; Akiyama, Y.; Kataoka, K.; Winnik, F. M. *Macromolecules* **2004**, *37*, 2556.
(42) Alexandridis, P.; Alan Hatton, T. *Colloids Surf., A* **1995**, *96*, 1.
(43) Riess, G. *Prog. Polym. Sci.* **2003**, *28*, 1107.
(44) Hoogenboom, R.; Schlaad, H. *Polymers* **2011**, *3*, 467.
(45) Diehl, C.; Dambowsky, I.; Hoogenboom, R.; Schlaad, H. *Macromol. Rapid Commun.* **2011**, *32*, 1753.
(46) Zhang, L.; Eisenberg, A. *J. Am. Chem. Soc.* **1996**, *118*, 3168.

## ■ NOTE ADDED AFTER ASAP PUBLICATION

This paper was published ASAP on January 14, 2016, with text errors in the Materials section. The corrected version was reposted on January 15, 2016.


DOI: 10.1021/acs.macromol.5b02481
*Macromolecules* XXXX, XXX, XXX−XXX